

Mode-locking of 2 μm Tm,Ho:YAG laser with GaInAs and GaSb-based SESAMs

Kejian Yang,^{1,2,*} Dirk Heinecke,¹ Jonna Paajaste,³ Christoph Kölbl,¹ Thomas Dekorsy,¹ Soile Suomalainen,³ and Mircea Guina^{3,4}

¹Department of Physics and Center of Applied Photonics, University of Konstanz, 78457 Konstanz, Germany

²School of Information Science and Engineering, Shandong University, Jinan, 250100, China

³Tampere University of Technology, Korkeakoulunkatu 3, 33720 Tampere, Finland

⁴RefleKron Ltd., Muotialankuja 5 C5, 33800 Tampere, Finland

*k.j.yang@sdu.edu.cn

Abstract: We have investigated passive mode-locking of Tm,Ho:YAG lasers with GaInAs- and GaSb-based semiconductor saturable absorber mirrors (SESAMs). With a GaInAs-based SESAM, stable dual-wavelength mode-locking operation was achieved at 2091 nm and 2097 nm, generating pulses with duration of 56.9 ps and a maximum output power of 285 mW. By using the GaSb-based SESAMs, we could generate mode-locked pulses as short as 21.3 ps at 2091 nm with a maximum output power of 63 mW. We attribute the shorter pulse duration obtained with the GaSb SESAMs to the ultrafast recovery time of the absorption and higher nonlinearity compared to standard GaInAs SESAMs.

©2013 Optical Society of America

OCIS codes: (140.3070) Infrared and far-infrared lasers; (140.4050) Mode-locked lasers; (140.5680) Rare earth and transition metal solid-state lasers; (140.7090) Ultrafast lasers; (160.6000) Semiconductor materials.

References and links

1. R. R. Gattass and E. Mazur, "Femtosecond laser micromachining in transparent materials," *Nat. Photonics* **2**(4), 219–225 (2008).
2. K. Schepler, B. Smith, F. Heine, and G. Huber, "Passive Q-switching and mode locking of 2- μm lasers," *Proc. SPIE* **1864**, 186–189 (1993).
3. R. C. Sharp, D. E. Spock, N. Pan, and J. Elliot, "190-fs passively mode-locked thulium fiber laser with a low threshold," *Opt. Lett.* **21**(12), 881–883 (1996).
4. S. Kivistö, T. Hakulinen, M. Guina, and O. G. Okhotnikov, "Tunable Raman Soliton Source Using Mode-Locked Tm–Ho Fiber Laser," *IEEE Photon. Technol. Lett.* **19**(12), 934–936 (2007).
5. Q. Wang, J. Geng, T. Luo, and S. Jiang, "Mode-locked 2 μm laser with highly thulium-doped silicate fiber," *Opt. Lett.* **34**(23), 3616–3618 (2009).
6. M. A. Solodyankin, E. D. Obratsova, A. S. Lobach, A. I. Chernov, A. V. Tausenev, V. I. Konov, and E. M. Dianov, "Mode-locked 1.93 μm thulium fiber laser with a carbon nanotube absorber," *Opt. Lett.* **33**(12), 1336–1338 (2008).
7. A. A. Lagatsky, F. Fusari, S. Calvez, J. A. Gupta, V. E. Kisel, N. V. Kuleshov, C. T. A. Brown, M. D. Dawson, and W. Sibbett, "Passive mode locking of a Tm,Ho:KY(WO₄)₂ laser around 2 μm ," *Opt. Lett.* **34**(17), 2587–2589 (2009).
8. A. A. Lagatsky, X. Han, M. D. Serrano, C. Cascales, C. Zaldo, S. Calvez, M. D. Dawson, J. A. Gupta, C. T. A. Brown, and W. Sibbett, "Femtosecond (191 fs) NaY(WO₄)₂ Tm,Ho-codoped laser at 2060 nm," *Opt. Lett.* **35**(18), 3027–3029 (2010).
9. A. A. Lagatsky, F. Fusari, S. Calvez, S. V. Kurilchik, V. E. Kisel, N. V. Kuleshov, M. D. Dawson, C. T. A. Brown, and W. Sibbett, "Femtosecond pulse operation of a Tm,Ho-codoped crystalline laser near 2 microm," *Opt. Lett.* **35**(2), 172–174 (2010).
10. A. A. Lagatsky, O. L. Antipov, and W. Sibbett, "Broadly tunable femtosecond Tm:Lu₂O₃ ceramic laser operating around 2070 nm," *Opt. Express* **20**(17), 19349–19354 (2012).
11. A. Härkönen, J. Paajaste, S. Suomalainen, J. P. Alanko, C. Grebing, R. Koskinen, G. Steinmeyer, and M. Guina, "Picosecond passively mode-locked GaSb-based semiconductor disk laser operating at 2 μm ," *Opt. Lett.* **35**(24), 4090–4092 (2010).
12. W. B. Cho, A. S., J. H. Yim, S. Y. Choi, S. Lee, F. Rotermund, U. Griebner, G. Steinmeyer, V. Petrov, X. Mateos, M. C. Pujó, J. J. Carvajal, M. Aguiló, and F. Díaz, "Passive mode-locking of a Tm-doped bulk laser near 2 μm using a carbon nanotube saturable absorber," *Opt. Express* **17**, 11007–11012 (2009).

13. K. J. Yang, H. Bromberger, H. Ruf, H. Schäfer, J. Neuhaus, T. Dekorsy, C. V. B. Grimm, M. Helm, K. Biermann, and H. Künzel, "Passively mode-locked Tm:Ho:YAG laser at 2 μm based on saturable absorption of intersubband transitions in quantum wells," *Opt. Express* **18**(7), 6537–6544 (2010).
14. I. A. Denisov, N. A. Skoptsov, M. S. Gaponenko, A. M. Malyarevich, K. V. Yumashev, and A. A. Lipovskii, "Passive mode locking of 2.09 μm Cr,Tm,Ho:Y₃Sc₂Al₃O₁₂ laser using PbS quantum-dot-doped glass," *Opt. Lett.* **34**(21), 3403–3405 (2009).
15. J. Ma, G. Q. Xie, W. L. Gao, P. Yuan, L. J. Qian, H. H. Yu, H. J. Zhang, and J. Y. Wang, "Diode-pumped mode-locked femtosecond Tm:CLNGG disordered crystal laser," *Opt. Lett.* **37**(8), 1376–1378 (2012).
16. A. Harkonen, C. Grebing, J. Paajaste, R. Koskinen, J. P. Alanko, S. Suomalainen, G. Steinmeyer, and M. Guina, "Modelocked GaSb disk laser producing 384 fs pulses at 2 μm wavelength," *Electron. Lett.* **47**(7), 454–456 (2011).
17. F. Schättiger, D. Bauer, J. Demsar, T. Dekorsy, J. Kleinbauer, D. H. Sutter, J. Puustinen, and M. Guina, "Characterization of InGaAs and InGaAsN semiconductor saturable absorber mirrors for high-power mode-locked thin-disk lasers," *Appl. Phys. B* **106**(3), 605–612 (2012).
18. J. Paajaste, S. Suomalainen, R. Koskinen, A. Härkönen, G. Steinmeyer, and M. Guina, "Dynamic properties of 2 μm GaSb-based semiconductor saturable absorber mirrors," the 29th North American Molecular Beam Epitaxy Conference, October 14–17, 2012, Georgia, USA; proceeding to be published as a special issue of the *Journal of Vacuum Science and Technology*.
19. T. Y. Fan, G. Huber, R. L. Byer, and P. Mitzscherlich, "Continuous-wave operation at 2.1 μm of a diode-laser-pumped, Tm-sensitized Ho:Y₃Al₅O₁₂ laser at 300 K," *Opt. Lett.* **12**(9), 678–680 (1987).

1. Introduction

Ultrashort laser sources operating near 2 μm eye-safe spectral range are of special importance for applications in light detection and ranging (LIDAR), frequency metrology, time-resolved spectroscopy, laser microsurgery, free space optical communication, optical pumping of solid state lasers and optical parametric oscillators (OPOs) in mid- and far-infrared spectral regions. Other important applications include material processing of plastics and 3-D microstructuring of semiconductor [1]. Typical ultrafast laser operating at 2 μm make use of passive mode-locking mechanisms and gain provided by Tm³⁺- and Tm³⁺-Ho³⁺-doped crystalline host or optical fibre. The mode-locking driving force is ensured by saturable absorbers fabricated from semiconductor materials, typically in the form of semiconductor saturable absorber mirrors (SESAMs), carbon-nanotubes or novel materials such as graphene.

First demonstration of a passively mode-locked laser at 2 μm was based on using a GaInAs SESAM [2]. A multiple quantum-well (MQW) GaInAs SESAM was also used to mode-lock a thulium-doped silica fiber laser and generated 190 fs pulses [3]. Subsequently, GaSb-based SESAMs [4, 5] and single walled carbon nanotubes (SWCNTs) [6] were successfully used in Tm³⁺- and Tm³⁺-Ho³⁺-doped ultrashort fiber lasers. Saturable absorption mode-locking had not been demonstrated in Tm³⁺- and Tm³⁺-Ho³⁺-doped bulk lasers until 2009. Since then a large variety of saturable absorbers, such as GaSb-based SESAMs [7–11], SWCNTs [12], intersubband transitions (ISBTs) in quantum wells [13], PbS quantum dots [14], and graphene [15] have been employed in 2 μm bulk lasers. Amongst these, SESAMs, have gained precedence for mode-locking a large variety of bulk laser because of their simplicity of use and fabrication, reliability, and capability to tailor their parameters to satisfy specific laser requirements, i.e. absorption band, contrast, non-saturable losses, absorption recovery time.

More recently, ps- and sub-ps pulses at around 2 μm have been also obtained using a GaSb-based gain mirrors and SESAMs used in a semiconductor disk laser cavity [11, 16]. In these measurements it has been reported that GaSb SESAMs exhibit a much faster absorption recovery, i.e. with sub-ps and ps characteristic times, compared to standard GaAs-based or InP-based SESAMs. These standard materials exhibit carrier life-times in the range of hundreds of ps or even ns and require the use of more complicated fabrication processes, such as low-temperature growth, doping of the active region, or ion-implantation in order to be suitable for mode-locking. At the same time these measures could result in degradation of other important parameters such as the non-saturable loss. These limitations continue to motivate the development of alternative SESAM materials that exhibit short absorption recovery times [17].

Besides the recently reported ultrafast absorption recovery time for as-grown GaInSb/GaSb QWs [11, 18], the GaSb SESAMs offers other attractive features compared with GaInAs/GaAs MQWs operating at 2 μm . Firstly, GaInSb/GaSb layers are nearly lattice matched, which in turn enable to tailor the nonlinear properties by simply changing the amount of QWs without detrimental effects on to material quality and non-saturable losses. Moreover, GaSb SESAMs incorporate lattice-matched GaSb/AlAsSb distributed Bragg reflectors (DBRs), which enable high reflectivity with only a small amount of pairs and exhibit an exceptionally broad reflection band of about 300 nm.

In this paper, we demonstrate the fabrication of GaSb-based SESAM and its application in a mode-locked Tm,Ho:YAG laser at 2 μm . Compared with the commercial GaInAs-based SESAM and GaInAs/AlAsSb based ISBTs semiconductor saturable absorber, the GaSb-based SESAM showed potential ability to produce much shorter mode-locked pulse. We attribute this to the intrinsic faster absorption recovery time and higher nonlinearity. We note here that unlike the InGaAsSb/GaSb reported previously in connection mode-locking of solid-state lasers, our SESAMs incorporate as-grown high-quality QWs which were not ion-irradiated [8, 10].

2. Fabrication and spectra of GaSb-SESAMs

The GaSb-based SESAMs were grown using a conventional molecular beam epitaxy system equipped with crackers for generation of Sb_2 and As_2 from Sb_4 and As_4 sources. The DBR consisted of 18.5 pairs of lattice-matched AlAsSb/GaSb layers ensuring a reflectivity of about 99.9%. The stop-band was centered at around 2000 nm. The absorbing region comprised 8-nm thick $\text{Ga}_{0.71}\text{In}_{0.29}\text{Sb}$ QWs with a thickness of 8 nm, which were embedded within GaSb layers and provided near-resonate operation at the laser wavelength. In order to assess the influence of the SESAM properties on laser performance we used two SESAMs, which were otherwise similar except for the number of QWs; a first structure comprised 2 QWs while the second one comprised 3 QWs. We note here that the 3 QWs structure is the same with the one used in Ref [16] for generation of 380 fs pulses. The absorption recovery time of the GaInSb QWs had a double-exponential decay characteristic with a fast time component of ~ 0.5 ps and a slow component of ~ 9 ps [11].

A commercial SESAM (Batop Inc.) based on an anti-resonant design with a 50 nm thick $\text{Ga}_{0.33}\text{In}_{0.67}\text{As}$ /GaAs absorber layer, corresponding to a saturation fluence of 70 $\mu\text{J}/\text{cm}^2$ and a modulation depth of about 0.8% at 2000 nm, was employed for comparison with the GaSb-based SESAMs. The GaInAs-SESAM exhibited an absorption recovery time of ~ 10 ps. The non-saturable loss of the GaInAs-SESAM was about 0.7%. Figure 1 shows the normalized low-intensity reflectivity spectra of the samples measured by Fourier transform infrared spectroscopy. The GaInAs SESAM shows a broader and flatter reflectivity curve than the SESAM samples based on GaSb, however we should note that in this case the structure does not incorporate a monolithic DBR but a dielectric reflector which is deposited post-growth. Figure 1 reveals also that the absorption available by using GaInSb QWs is higher than for GaInAs structure; this is typical for resonant structures but in this case the overall thickness of the absorber might be limited by the high lattice mismatch of the QWs and GaAs substrate). Secondly, it is also important to note that at the wavelengths resonant with the band-gap, there is a significant difference in absorption between the GaSb SESAMs with 2 QWs and 3 QWs; as expected the 3 QW samples exhibit higher absorption.

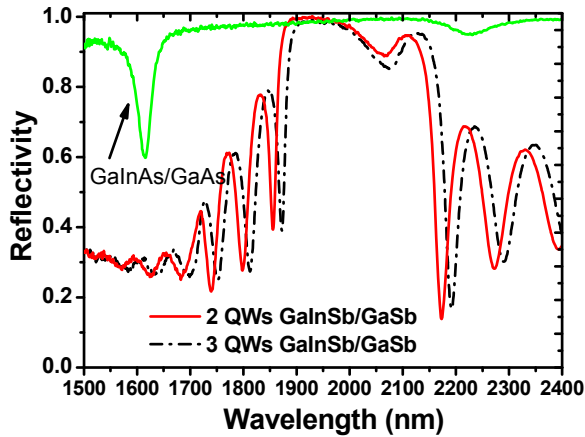


Fig. 1. Low-intensity reflectivity spectra of GaInAs SESAM and 2 QWs and 3 QWs GaSb based SESAMs.

3. Experimental setup and results

The schematic of the laser setup is shown in Fig. 2. The pump source was a continuous wave (CW) linearly polarized Ti:sapphire laser tunable from 726 nm to 859 nm. The employed pump wavelength was 780.5 nm. A half wave plate with antireflection coated at 780 nm was used to change the polarization of the pump light. A lens with a focal length of 75 mm focused the pump light into a Brewster angled Tm, Ho:YAG crystal. The crystal was 5 mm-long and was doped with 5at.-%-Tm³⁺, 0.4at.-%-Ho³⁺:YAG crystal with Brewster angle cut was employed as the gain medium. The Tm,Ho:YAG crystal was wrapped in Indium foil and mounted in a copper holder with water cooled to be 12 °C. Mirrors M₁ and M₂ had the same radii of curvature of 100 mm and reflectivity of 99.9% from 1820 to 2150 nm. The front surface of mirror M₁ was also anti-reflection coated at the wavelengths of 750-850 nm with a reflectivity less than 0.25%. Flat mirror M₃ and concave mirrors M₄, M₅ and M₆ with respective curvature radii of 30 mm, 50 mm and 100 mm were all high reflectivity coated from 1820 to 2150 nm (reflectivity >99.9%). All the cavity mirrors except the output couplers had group delay dispersion (GDD) of ~100 fs² in the 1820 nm to 2150 nm spectral region. To compensate the astigmatism induced by the folding mirrors and the Brewster angle cut laser crystal, the folded angle of the mirrors was 5°. When estimated with ABCD matrix propagation theory, the laser mode waist radii in the laser crystal were 37 μm and 43 μm in sagittal and tangential planes, respectively. The beam waist radii at the position of saturable absorber were about 73 μm in both sagittal and tangential planes.

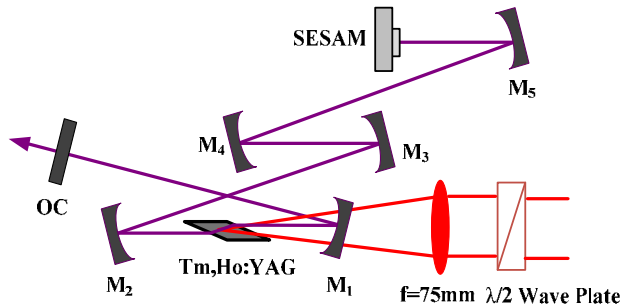


Fig. 2. CW and mode-locked Tm,Ho:YAG laser setup.

First we measured the CW characteristics using a plane mirror high reflectivity coated at 2 μm instead of SESAM and output couplers with transmissions of $T = 1\%$ (1820nm - 2150 nm, $\pm 0.2\%$) and 2% (1950 nm-2150 nm, ± 0.3). With the output coupler of $T = 1\%$, the laser operated at 2123 nm after reaching the threshold absorbed pump power of 248 mW. When the absorbed power reached 528 mW, the laser started to run in dual wavelength regime at 2091 nm and 2123 nm. By increasing the absorbed pump power to 1.621 W, tri-wavelength operation was obtained at 2091 nm, 2097 nm, and 2123 nm; the corresponding spectrum is shown in Fig. 3(a). According to Ref [19], we can see that all the emission wavelengths listed above are located at respective fluorescence peaks of the Tm, Ho:YAG crystal. Since all the intracavity mirrors were coated in a spectral range from 1950 to 2150 nm, different modes reached the oscillation thresholds, when the pump intensity was high enough. Therefore dual- and triple- wavelength operation could be realized. When the absorbed pump power reached around 2 W, one oscillating mode was diminished while another was enhanced due to the intracavity mode competitions, which resulted in a decrease of output slope efficiency. In the case with the output coupler of $T = 2\%$, the laser started to oscillate at 2097 nm at a threshold absorbed pump power of 218 mW. When the absorbed pump power reached 405 mW, the laser ran in stable dual-wavelength operation at 2091 nm and 2097 nm, as shown in Fig. 3(b). The total output power characteristics are shown in Fig. 4 with slope efficiencies of 22.2% and 28.2% for output couplers of $T = 1\%$ and 2%, respectively.

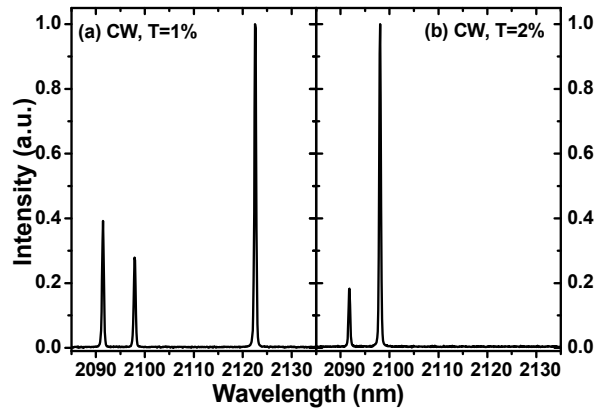


Fig. 3. Spectrum of cw Tm, Ho:YAG laser with output coupler of (a) $T = 1\%$, (b) $T = 2\%$.

Using the GaInAs SESAM we achieved passive mode-locking operation of Tm, Ho:YAG laser. A 1 GHz bandwidth digital oscilloscope (DPO 5104, Tektronix Inc.) and a 60 MHz bandwidth extended-GaInAs PIN photodiode (G8423, Hamamatsu Inc.) were used to monitor the mode-locked pulse train leaking from mirror M_3 to optimize the stability of mode-locking operation. With the output couplers of $T = 1\%$ and 2%, the laser operation turned from stable into Q-switched mode-locking and then into stable mode-locking with spectra centered at 2091 nm at the absorbed pump power of 978 mW and 720 mW, respectively. When the incident pump power increased, the laser operated in stable dual-wavelength mode-locking at 2091 nm and 2097 nm. The stable mode-locking output powers are shown in Fig. 4 with slope efficiencies of 8.3% and 12.6%, respectively for output couplers of $T = 1\%$ and 2%, with which maximum output powers of about 195 mW and 285 mW were obtained under stable dual-wavelength stable mode-locking operation, respectively.

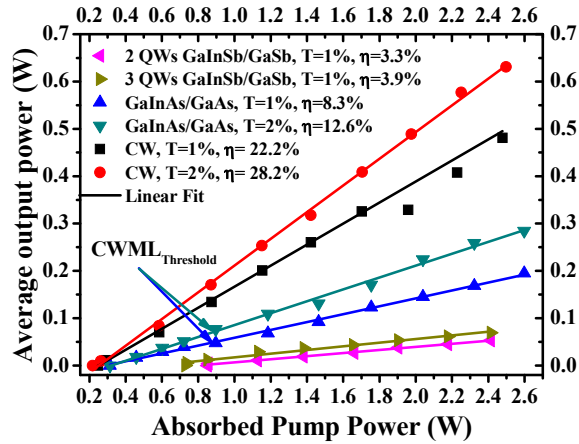


Fig. 4. Output power of cw and mode-locked Tm,Ho:YAG laser

The first beat note of the radio frequency (RF) spectrum was recorded by a spectrum analyzer with a bandwidth of 13.2 GHz and a resolution bandwidth of 1 kHz (E4405B, Agilent Inc.). The RF spectrum obtained under a span of 50 kHz shows a clean peak at the repetition rate of about 107 MHz without side peaks, which exactly agrees with the roundtrip time of the cavity and reveals stable continuous wave mode-locking operation of the laser as well as the absence of Q-switching instabilities. In addition, the 1GHz wide-span RF measurement indicated the single pulse operation of the mode-locked Tm, Ho:YAG laser, as shown inset of Fig. 5.

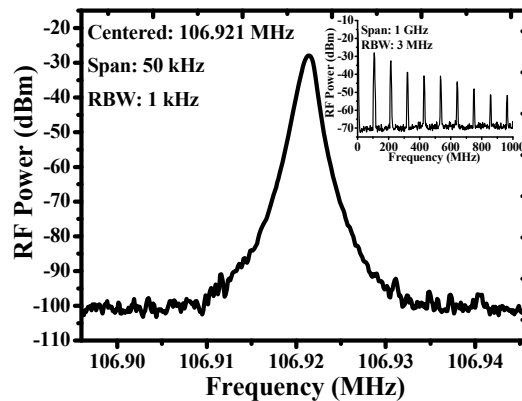


Fig. 5. RF spectrum of continuous wave mode-locked Tm,Ho:YAG laser. RBW: resolution bandwidth.

To measure the mode-locked pulse duration, a collinear autocorrelation setup using second harmonic generation with a PPLN crystal was employed. The pulse duration of was estimated to be 56.9 ps by assuming a sech^2 pulse shape as shown in Fig. 6(a). The corresponding optical spectrum with FWHM of 0.6 nm was measured by a laser spectrometer with a resolution bandwidth of 0.4 nm (APE WaveScan, APE Inc.), which is shown in Fig. 6(b). The pulse duration and spectrum obtained here are very similar with our previous results obtained with the ISBTs quantum wells based saturable absorber [13].

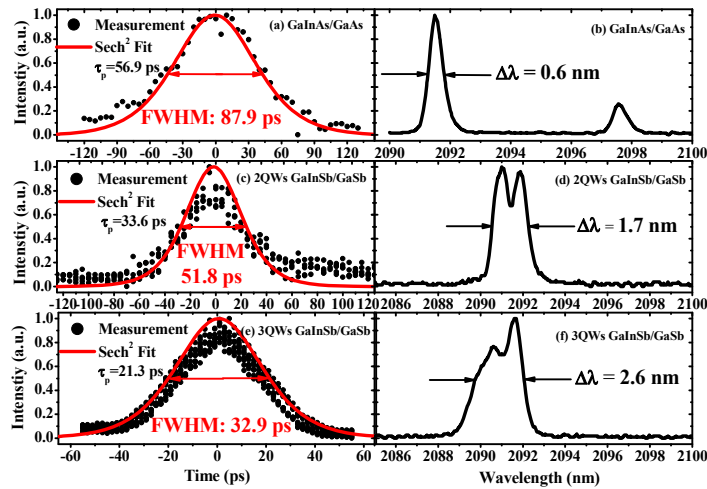


Fig. 6. Autocorrelation signal and spectra from mode-locked Tm,Ho:YAG laser.

For both GaSb-based SESAMs the stable mode-locking operations was achieved at 2091 nm by carefully adjusting the cavity mirrors and positions of the SESAMs (for $T = 1\%$ output coupler). In comparison with the GaInAs SESAM, the output powers with the GaSb SESAMs under stable mode-locking operation were much lower, as revealed in Fig. 4. The maximum output powers for the 2 QWs and 3 QWs SESAMs were 53 mW and 63 mW, with corresponding slope efficiencies of about only 3.3% and 3.9%, respectively. We attributed this to higher absorption of GaSb-SESAM samples combined with an absorption recovery time shorter than the pulse duration, and higher non-saturable losses caused by the fact that the DBR stop-band was not aligned with the lasing wavelength. Moreover, as it can be seen in Fig. 1, at the longest wavelength edge of the DBR stop-band the reflectivity for the 3 QWs SESAM is higher than the reflectivity for the 2 QWs SEASM. This has been caused by a slight blue-shift of the central stop-band wavelength for the 2 QWs structures occurring during the growth. Therefore, when fully saturated we do expect that the reflectivity of the 3 QWs structure would be slightly higher than the one for the 2 QWs structure, explaining the slight difference in the output power for the two cases. The threshold pump powers for stable mode-locking were almost the same with the lasing thresholds for both 2 QWs and 3 QWs GaSb-based SESAMs, corresponding to the fluences of $25.1 \mu\text{J}/\text{cm}^2$ and $33.5 \mu\text{J}/\text{cm}^2$ respectively. This indicates a lower saturation fluence than for the GaInAs SESAM. Most important, we observed the changes in pulse durations and emission spectra. With the 2 QWs SESAM, we obtained 33.6 ps stable mode-locked pulses with a corresponding spectrum bandwidth of 1.7 nm, while mode-locked pulses as short as 21.3 ps and a corresponding bandwidth of 2.6 nm were obtained for the higher nonlinearity SESAM incorporating 3 QWs; to the best of our knowledge these are the shortest pulses achieved so far from a Tm,Ho:YAG bulk laser. The autocorrelation signals and spectra are shown in Fig. 6(c) to 6(f). Obviously the time bandwidth product (TBP) was larger than the transform limited value of 0.314 for Sech² shaped pulse. However, the insertion loss induced by the silicon prism pair used to compensate intracavity dispersions prevented the oscillation of the mode-locked Tm,Ho:YAG laser, so we did not know the pulse duration with dispersion compensated. By shifting the DBR stop-band to around 2100 nm to increase the lasing efficiency and compensating the intracavity dispersions, the pulse duration from the mode-locked Tm,Ho:YAG laser is expected to be further shortened into the range of several picoseconds.

4. Conclusion

In conclusion, we have compared the performance of passively mode-locked Tm,Ho:YAG lasers employing GaInAs and GaInSb SESAMs. When using a SESAM comprising three GaInSb/GaSb QWs, we demonstrated pulses as short as 21.3 ps, which were two times shorter than for the case of GaInAs SESAM. Compared to GaAs SESAMs, the GaInSb-based QWs exhibit sub-ps recovery time for as-grown high quality structures and they are nearly lattice-matched to the substrates for the 2 μ m wavelength range – in turn this brings more flexibility for designing the optical properties of the SESAM. Our goal was to reveal these benefits by providing a direct comparison between the performance of GaAs and GaSb SESAMs operating in Tm,Ho:YAG lasers. Understanding the behavior of GaSb SESAMs is of general interest as this material system is able to cover the highly interesting wavelength region from 2 to 3 μ m. Further optimization of the GaSb-based SESAM and compensation of the intracavity dispersions, are expected to lead to the generation of even shorter pulses.

Acknowledgments

This work was supported by the Ministry of Science, Research and the Arts of Baden-Württemberg, National Natural Science Foundation of China (61008024), Research Award Fund for Outstanding Middle-aged and Young Scientist of Shandong Province (BS2011DX022), Independent Innovation Foundation of Shandong University, IIFSDU (2012JC025). Kejian Yang acknowledges support from Alexander-von-Humboldt Foundation. We thank Ernst Heumann and Guenter Huber from University of Hamburg for providing the Tm,Ho:YAG crystal.